Science of the Total Environment 894 (2023) 164931

Contents lists available at ScienceDirect

Science of the Total Environment

journal homepage: www.elsevier.com/locate/scitotenv

An index for inferring dominant transport pathways of solutes and sediment: Assessing land use impacts with high-frequency conductivity and turbidity sensor data

Amirreza Zarnaghsh, Admin Husic *

Department of Civil, Environmental and Architectural Engineering, University of Kansas, United States of America

HIGHLIGHTS

- Urbanization enhances hydrologic connectivity of salt to the stream network.
- Urbanization adds complexity to sediment delivery pathways during storms.
- New index to quantify the temporal coherence of runoff and sediment delivery.

GRAPHICAL ABSTRACT

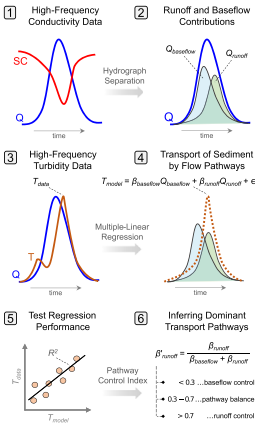

ARTICLE INFO

Editor: Ouyang Wei

Keywords:
Sediment transport
Runoff
Baseflow
Hysteresis
Hydrologic connectivity
Freshwater salinization

ABSTRACT

Land use change threatens aquatic ecosystems through freshwater salinization and sediment pollution. Effective river management requires an understanding of the dominant hydrologic pathways of sediment and solute delivery. To address this, we applied hysteresis analysis, hydrograph separation, and linear regression to hundreds of events across a decade of specific conductance and turbidity data from three streams along a rural-to-urban gradient. Thereafter, we developed an index (β'_{runoff}) to quantify the relative influence of surface runoff to event-scale suspended sediment generation, where a value of '1' indicates complete alignment of suspended sediment generation with the temporal structure of runoff whereas '0' indicates total alignment with baseflow. Solute hysteresis results showed a predominance of dilution for the rural and mixed-use streams irrespective of road salt presence. On the other hand, urban stream behavior shifted from dilution to flushing following salt application, which was largely driven by greater runoff coefficients and the connectivity of distal solutes to the stream corridor. The newly developed index (β'_{runoff}) indicated that suspended sediment dynamics were more aligned with runoff in all three streams: rural stream ($\beta'_{runoff} = 0.70$), mixed stream ($\beta'_{runoff} = 0.57$), and urban stream ($\beta'_{runoff} = 0.64$). The relative importance of baseflow to sediment generation grows slightly in urbanizing streams, as impervious surfaces disconnect upland sediment, which would otherwise transport with runoff, while piston-flow baseflow erodes exposed streambanks. Our findings emphasize the need to consider the impact of human modification of the landscape on solute and sediment transport in freshwater systems for effective water quality management. Further, our β'_{runoff} index provides a useful tool for assessing the relative

* Corresponding author at: 2134B Learned Hall, University of Kansas, Lawrence, KS 66045, United States of America.
E-mail address: ahusic@ku.edu (A. Husic).

http://dx.doi.org/10.1016/j.scitotenv.2023.164931
Received 28 February 2023; Received in revised form 13 June 2023; Accepted 14 June 2023
Available online 20 June 2023

influence of surface runoff on event-scale solute or sediment generation in streams, supporting river management and conservation efforts.

1. Introduction

Increasing salinity and sediment pollution are two of the most critical issues threatening freshwater habitats across the globe (Chapman et al., 2014; Kaushal et al., 2018; Iglesias, 2020). The annual economic costs due to their negative impacts are estimated to be in billions of U.S. dollars and include ecological degradation (Vercruysse et al., 2017), hindered water supply (Rahmani et al., 2018), and damage to crops (Schuler et al., 2019). While natural phenomena, including weathering and soil erosion, and agricultural activities, such as tillage and tile drainage, contribute to sediment and solute loading to streams (Fitzpatrick et al., 2007; Michalek et al., 2021), urbanization has accelerated this loading by increasing peak discharge (Russell et al., 2018), wastewater contribution (Ledford and Toran, 2019), road-salt application (Lakoba et al., 2020), and connectivity of sediment sources (Zarnaghsh and Husic, 2021). Despite the recognized impacts of urbanization on riverine water quality, uncertainty remains regarding the specific mechanisms by which human activity alters the delivery of sediment and solutes to streams (Oswald et al., 2023). Understanding these changes is vital as two-thirds of the world population is projected to live in urban areas by 2050 (Bettencourt et al., 2018), nearly doubling current-day urban densities and bringing new water resources challenges for the future.

Storm events are recognized as the key moments of sediment and solute mobilization to streams (Vaughan et al., 2017; Musolff et al., 2021). However, analyzing land-use pattern effects on transport processes during storms is challenging because event concentration-discharge relationships have high temporal variability and are driven by hydrological and climatic variables such as precipitation, storm intensity, and antecedent conditions (Namugize et al., 2018; Zimmer et al., 2019). Further, human disturbances add to the existing natural complexity by creating new sources (e.g., wastewater treatment plants) and hydrologic pathways (e.g., storm sewers and drainage ditches), which in turn contribute to additional heterogeneity in watershed-scale response to storms (Long et al., 2017; Aguilera and Melack, 2018; Lakoba et al., 2020). For example, the application of road salt in urban areas to remove snow from roadways and improve driver safety is a common practice in cold regions. However, this practice has significant environmental implications as runoff and infiltration of the applied salt can lead to lasting impacts on riverine water quality (Daley et al., 2009; Lakoba et al., 2020). In addition to hydroclimate and land use controls, transport dynamics are significantly dependent on topography, geology, and soil type (Koenig et al., 2017; Wymore et al., 2019). To effectively isolate the specific impacts of land use on solute and sediment transport, it is imperative to minimize the variability of other hydrologic drivers to limit the overprinting of one set of transport controls on another. Therefore, solute and sediment transport dynamics in an urbanizing landscape cannot be properly understood unless we have a long-term, detailed record of temporal variations in stream water quality during storm events.

With the advent of high-frequency aquatic sensors, such as turbidity and conductivity, we can now observe changes to stream water quality at physically and biochemically relevant time scales (Fig. 1; Rode et al., 2016; Burns et al., 2019). Sensors can resolve rapid changes in water quality, such as the initial increase in solutes at the early stages of a storm (termed the “first flush”), which may then be followed by rapid dilution of the same constituent during later parts of an event (Lawler et al., 2006; Demers et al., 2021). This asynchronous behavior between peak discharge and peak concentration of a water quality parameter is termed “hysteresis” and various numerical indices have been created to characterize hysteresis (Lloyd et al., 2016a; Zuecco et al., 2016). Analysis of hysteresis can help us to gain more insights into spatial and temporal dynamics of sediment and solute source availability and storage due to its inherent high temporal resolution and quantitative description of concentration-discharge relationships (Lloyd et al., 2016a, 2016b, Fovet et al., 2018). However, concentration-discharge methods have limitations that relate to the difficulty of interpreting transport processes for complicated hysteresis patterns, the scale dependency of hysteresis results on the size of the watershed, and the applicability of substituting time for space in interpreting results (Gao and Josefson, 2012; Sherriff et al., 2016). Therefore, further work is required to better understand the specific hydrologic pathways transporting the material, and how these pathways may be altered by urbanization.

Hydrologic pathways can broadly be separated into two components: runoff and baseflow (Cartwright and Miller, 2021). Baseflow (or “old” water) can be interpreted to refer to water stored in the watershed prior to a precipitation event whereas runoff (or “new” water) is usually considered as quick flow arriving to streams during and after a precipitation event (Waterman et al., 2022). The relative timing and magnitude of each flow component during a storm can be determined through end-member hydrograph separation. In particular, researchers have increasingly used specific conductance (SC) sensor data to determine the significance of surface runoff and baseflow to stormflow generation (Miller et al., 2014, 2017; Tunqui Neira et al., 2020; Nazari et al., 2021). Regarding land use effects, it

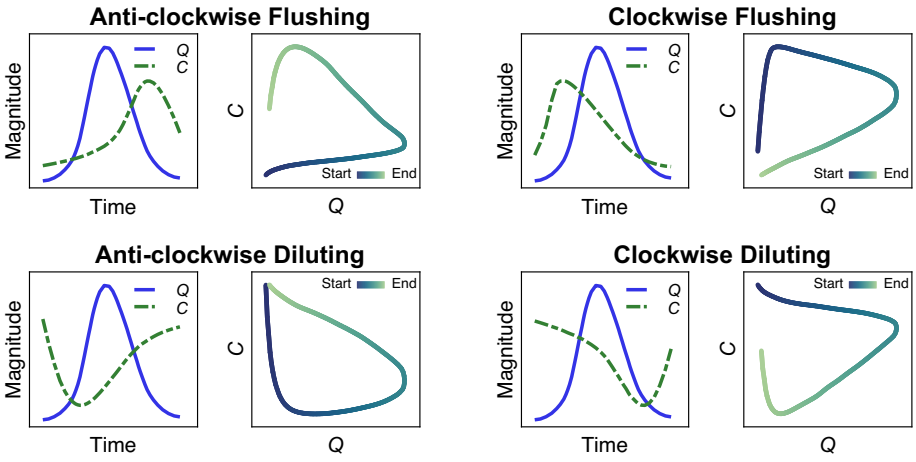

Fig. 1. A conceptual diagram of hysteresis and flushing dynamics between the discharge of water (*Q*) and the concentration of a solute or particle (*C*). The four plotted events are archetypal examples, real observations include a much broader variety of hysteresis patterns, such as figure-eight.

is well-recognized that expansion of impervious area drives up runoff contribution and that wastewater effluent discharges increase baseflow loading (Lakoba et al., 2020). However, less certain is how these flow alterations manifest in changing the dynamics by which sediments are generated within the basin and arrive to a monitoring outlet. While urban areas typically experience exacerbated streambank erosion (Cashman et al., 2018; Percich et al., 2022), it is uncertain whether that eroded bank material is transported by water of runoff or baseflow origin. Increases in suspended sediment concentrations during storm events, herein termed 'suspended sediment generation', could be evaluated by assessing the coincident rise in stream sediment concentration that is mirrored by an increase in the contribution of a particular hydrologic pathway, such as runoff or baseflow. To this end, coupling event-based hydrograph separation methods with high-frequency turbidity sensing across an urbanization gradient may help resolve these uncertainties.

Our main objective was to analyze the effects of land use on the dominant pathways of salinity and sediment generation in streams. We do this by investigating 1) solute flushing and dilution dynamics, 2) the relative significance of runoff versus baseflow to storm events, and 3) the role of runoff versus baseflow to fluvial sediment generation. We hypothesized that – because urbanization practices expose streambanks to erosion and limit upland sediment availability – baseflow would become a more important contributor to suspended sediment generation in urban streams. We tested this hypothesis on up to 12 years of high-frequency conductivity and turbidity data from three streams spanning a steep urbanization gradient. We performed hysteresis analysis to assess solute dynamics, end-member hydrograph separation to quantify new and old water components, and multiple linear regression to evaluate the relationship between water components and sediment loading. Lastly, we introduce a new quantitative index – β'_{runoff} – to describe the relative importance of runoff versus baseflow to sediment generation in a stream.

2. Study site and materials

2.1. Study site

Three watersheds in Johnson County, Kansas, USA, were selected as testbeds for our study as they exhibit large spatial variability in anthropogenic land use despite similar climatological and geomorphological settings (Fig. 2 and Table S1). From least-urban to most-urban, they are named Blue River, Mill Creek, and Indian Creek, which we refer to herein as Rural Stream, Mixed Stream, and Urban Stream, respectively. Rural Stream has a high degree of row cropping, riparian tree canopy cover, and animal pasture with relatively low impervious surfaces and roadway density as well as no wastewater treatment facility (WWTF) effluent. On the other hand, Urban Stream contains several WWTFs, is almost entirely urbanized, and has three-to-four times the impervious surface and roadway density of Rural Stream. Mixed Stream is a midpoint between the two contrasting land uses and contains features characteristic of both the urban and rural watersheds. The overall study region is characterized by a temperate climate with mean annual temperature and precipitation of 13.7 ± 0.4 °C and 958 ± 211 mm yr^{-1}, respectively. The range of elevation in the Rural, Mixed, and Urban Watersheds varies from 222 to 355 m, 247 m to 338 m, and 263 to 333 m, respectively, indicating a relatively low relief landscape. Although there are occasional steep slopes near stream channels, the average slope is considered gentle (3.5°) in all three watersheds. All

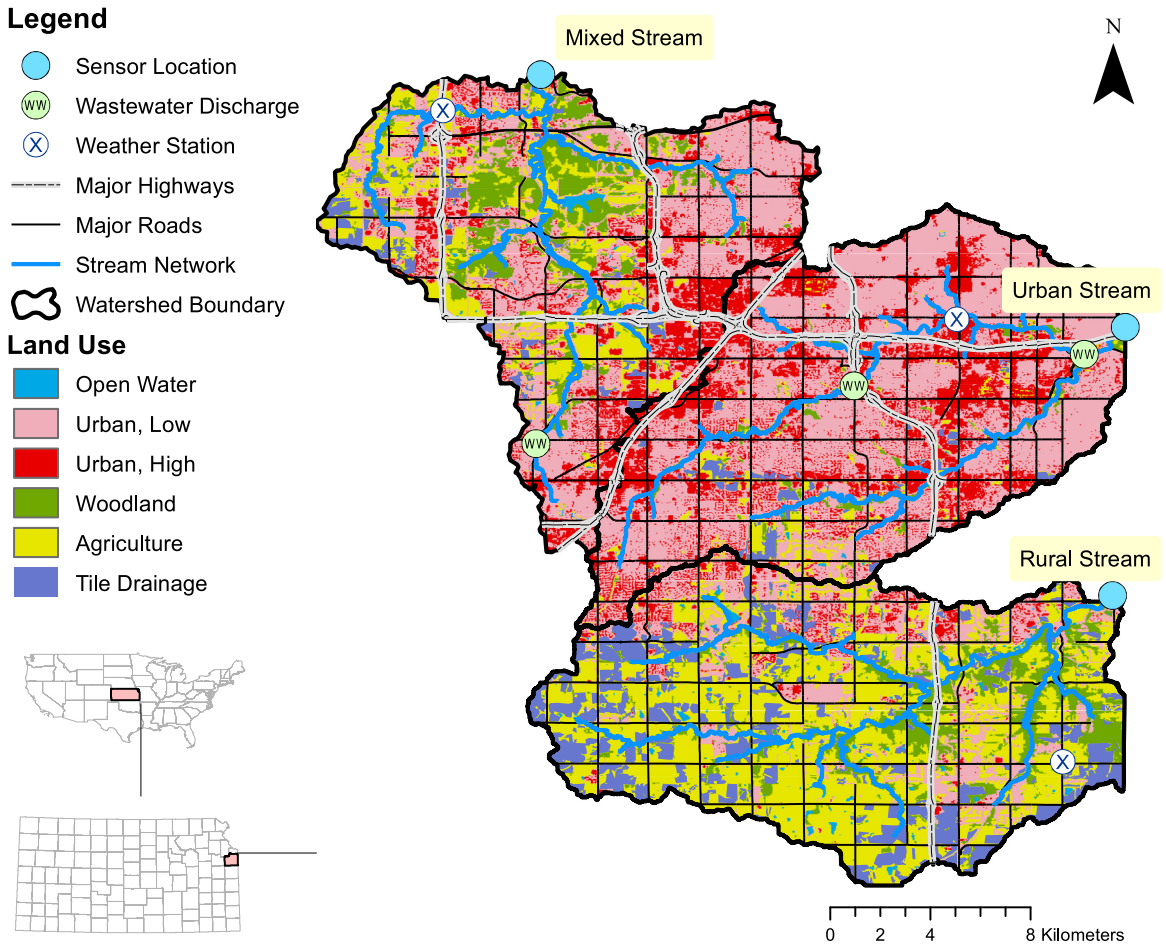

Fig. 2. The study site location within Johnson County, Kansas, USA. Land use, pour points, stream networks, roadways, weather stations, and wastewater discharges for the rural, mixed, and urban streams.

watersheds in Johnson County are underlain by relatively impermeable limestone and shale, which limits the infiltration of precipitation to groundwater in most parts of the catchments. As a result, the groundwater capacity is low, and stormflow mainly originates from overland or shallow subsurface flow (Lee and Ziegler, 2009). The soils in Johnson County typically consist of silt and silty clay loams that range from erosive to moderately erosive. Streambeds are generally composed of bedrock, gravel, and cobble, indicating that bedload is not a significant contributor to stream sediment. However, streambanks and upland soils, which are mostly composed of silt and silty clay loams, can contribute significantly to sediment yield.

2.2. Materials

Starting in 2002, the United States Geological Survey (USGS) began collecting 15-min high-frequency water quality data in Johnson County, including at the Rural Stream, Mixed Stream, and Urban Stream sites (Rasmussen and Gatotho, 2014). For this study, we used their discharge, specific conductance, and turbidity data over the course of twelve years (2002 to 2014). The extent of continuous data availability per site varies from 6 years in Mixed Stream to 10 years in Urban Stream. At each site, discharge was estimated using a piezometer whereas specific conductance and turbidity were measured using a YSI 6136 multiparameter sonde. The relationship between turbidity (FNU) and suspended sediment concentration (SSC) was verified by grab samples for each site (R^2 ranged between 0.80 and 0.90; Fig. S1).

To assess the influence of anthropogenic and natural features to solute and sediment dynamics, we retrieved several geospatial and temporal datasets. Road networks were extracted from the topologically integrated geographic encoding and referencing data set (United States Census Bureau, 2007). Road salt application dates and magnitudes were obtained from Johnson County Stormwater Management Program (SMP) and the daily wastewater discharges were acquired from the individual facilities (personal communication with SMP, 2022). Additionally, we employed the United States Forest Service (USFS) Tree Canopy Cover Dataset to determine the tree canopy coverage within a 200-m riparian buffer surrounding each stream's main channel. Lastly, precipitation data were retrieved from the closest gage to each stream's outlet using Johnson County StormWatch (StormWatch, 2020).

3. Methods

To achieve an understanding of the movement of solute and sediment through urbanizing basins, we leverage multiple high-frequency datasets and modeling approaches (Fig. S2). Briefly, road salt application dates, stream discharge, and high-frequency conductivity data inform our hysteresis and flushing results (Section 3.1). These results, together with hydroclimatological drivers and wastewater discharge, are inputs to our hydrograph separation model, providing insight into runoff and baseflow dynamics (Section 3.2). Lastly, we couple the hysteresis and hydrograph separation results with high-frequency turbidity data and multiple-linear regression modeling to determine the relative importance of runoff and baseflow to suspended sediment generation (Section 3.3).

3.1. High-frequency sensing of solute dynamics and hysteresis

To investigate the pathways of solute transport, we employed hysteresis and flushing analyses on high-frequency specific conductance data, which we use to infer general solute transport, for all storm events. First, we begin with our criteria for an event. In our definition, a storm event refers to a specific time interval that starts with a rise in water flow that is at least three times the initial baseflow and ends either when the water flow returns to the pre-event flow or when another storm event begins. We visually check each storm event to avoid false endpoints or erroneous readings. These criteria for storm identification were selected based on previous studies (Tang and Carey, 2017; Koenig et al., 2017; Liu et al., 2020). Each storm event can be visually classified into one of the following broad categories: clockwise-flushing, clockwise-diluting, anticlockwise-flushing, and anticlockwise-diluting (see Fig. 1). The first term in this classification indicates the type of hysteresis and is dependent on the relative solute concentrations that are observed on the rising versus the falling limb. Clockwise hysteresis usually indicates proximal solute sourcing or rapid mobilization, whereas anti-clockwise patterns suggest distal sources, longer transport times, or slower mobilization. The second term in the classification demonstrates whether the mobilization of solutes is source (diluting) or transport (flushing) limited. Following visual classification, we transformed the timeseries of each event into normalized discharge and concentration space to quantitatively estimate the magnitude of flushing and hysteresis. This process involves the following steps: 1) normalizing specific conductance and discharge by their respective ranges and 2) discretizing the normalized concentration and discharge into 5 % intervals over the rising and falling limbs of the hydrograph.

We calculated the Hysteresis Index (*HI*; Lloyd et al., 2016a) as the difference between the normalized concentration on the rising limb (X^{RL}) and the falling limb (X^{FL}) at corresponding flow intervals (i) as

$$HI_i = X_i^{RL} - X_i^{FL} \quad (1)$$

The possible values for *HI* range from −1 to +1 and the overall event *HI* was estimated by taking the mean of all calculated HI_i values for an event. Positive values ($HI > 0$; clockwise) are inferred to represent a solute source that is either rapidly mobilized or near to the measuring point. On the other hand, negative values ($HI < 0$; anticlockwise) suggest either a distal source of solute or one that is slowly mobilized. The magnitude of *HI* indicates the strength of this asynchronous behavior between specific conductance and discharge. We calculated the Flushing Index (*FI*) as the difference between the normalized concentration at the peak discharge ($X_{\max\ Q}$) versus the concentration at storm initiation ($X_{initial}$) as

$$FI = X_{\max\ Q} - X_{initial} \quad (2)$$

The possible values for *FI* range from −1 to +1, where negative values ($FI < 0$; dilution) indicate solute dilution and positive values ($FI > 0$; flushing) indicate solute mobilization during the rising limb of an event. Depending on the calculated *HI* and *FI* values, each event can be assigned to one of the four quadrants: clockwise-flushing, anticlockwise-flushing, anticlockwise-dilution, and clockwise-dilution.

To assess whether the timing of road salt application impacts the observed solute transport dynamics, we compared the distribution of *HI* and *FI* for (1) all events and for (2) events immediately following known road salt application. Events after brine application, termed 'brining events', were selected if they (1) occurred within 30 days of road salt application and (2) if their discharge exceeded 3 $m^3\ s^{-1}$ to ensure adequate potential for salt mobilization and transport. Significant differences in non-brining and brining events were assessed using the non-parametric Wilcoxon text ($\alpha = 0.05$). Lastly, we visually inspected the start of all storm events – brining and non-brining – to assess the presence and magnitude of the 'first flush' of solute. The first flush was defined as a rapid increase in specific conductance (> 10 μS cm^{-1}) on the rising limb of the hydrograph, which can suggest rapid transport of solute within the riparian corridor of a stream.

3.2. Hydrograph separation of runoff and baseflow

To investigate the timing and contribution of hydrologic pathways, such as runoff and baseflow, to the overall stream discharge, we employed specific conductance end-member mixing analysis (SC-EMMA) to storm events (Fig. 3). We ultimately arrive at three hydrologic pathways: runoff (Q_{runoff}), baseflow ($Q_{baseflow}$), and wastewater treatment facility effluent (Q_{wwtf}). When combined, $Q_{baseflow}$ and Q_{wwtf} constitute the pre-event flow ($Q_{pre\text{-}event}$) in a stream. First, a two-component hydrograph separation model was used to estimate the two unknowns (Q_{runoff} and $Q_{pre\text{-}event}$) from the following two equations:

$$Q_{total} = Q_{runoff} + Q_{pre\ -\ event} \quad (3)$$

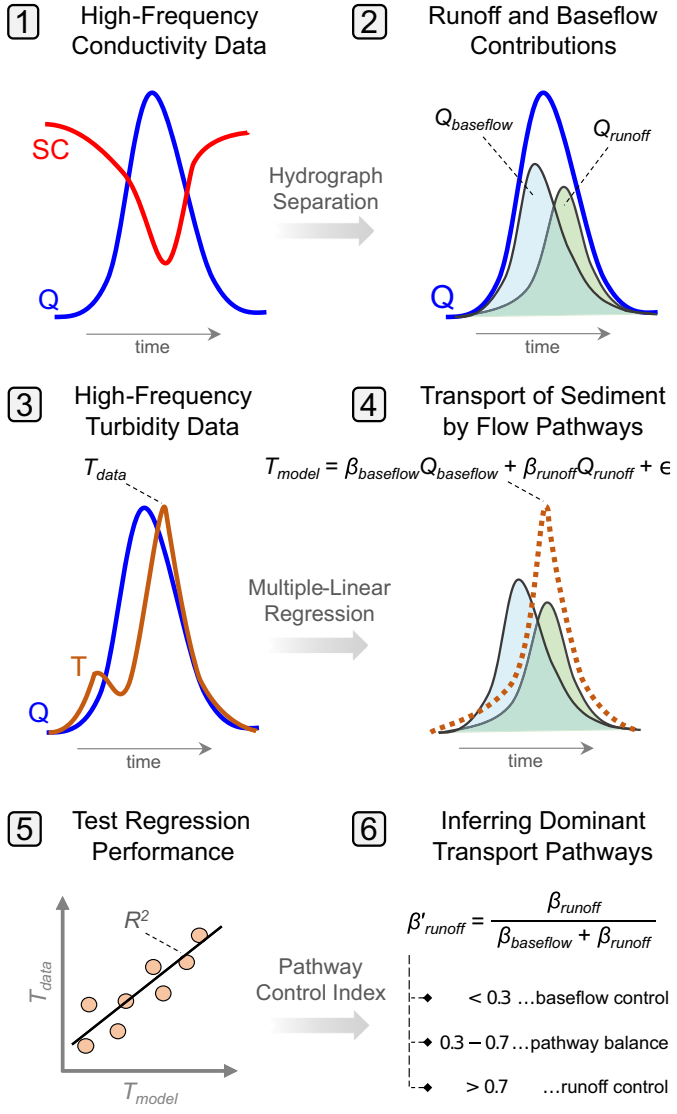

Fig. 3. A conceptual diagram of SC-EMMA hydrograph separation and multiple-linear regression for the identification of sediment transport by runoff and baseflow flow fractions. An example is presented where $\beta_{runoff} > \beta_{baseflow}$, i.e., the sediment signal in this event is more closely correlated with the runoff pathway.

$$Q_{total}SC_{total} = Q_{runoff}SC_{runoff} + Q_{pre-event}SC_{pre-event} \quad (4)$$

where Q_{total} is the combined stream flow ($m^3\ s^{-1}$), SC_{total} is the in-stream specific conductance, SC_{runoff} is the specific conductance of runoff, and $SC_{pre\text{-}event}$ is the specific conductance of pre-event water. We fixed SC_{runoff} to be 5 μS cm^{-1} in our analysis. This value was estimated using commonly reported values in the literature for rainwater and runoff, which range from 5 to 100 μS cm^{-1} (Cartwright and Miller, 2021). For $SC_{pre\text{-}event}$, we used the mean SC value for the 48-h period preceding the storm event. Eqs. (3) and (4) can be solved simultaneously to yield Q_{runoff} and $Q_{pre\text{-}event}$. Thereafter, $Q_{baseflow}$ can be determined by subtracting out Q_{wwtf} from $Q_{pre\text{-}event}$. Q_{wwtf} is known at all time periods as it is recorded by the wastewater treatment facilities.

In order to apply SC-EMMA, several assumptions have to be reasonably satisfied (Miller et al., 2014): 1) contributions from end-members other than Q_{runoff} and $Q_{pre\text{-}event}$ are negligible; 2) SC_{runoff} and $SC_{pre\text{-}event}$ are constant over the period of record; and 3) SC_{runoff} and $SC_{pre\text{-}event}$ are significantly different from one another. We satisfy the first assumption by lumping sources of water into two broadly defined end-members: runoff and pre-event flow. The second assumption is satisfied in two ways. First, while baseflow SC is time-variable over longer durations, we can reasonably expect it to remain constant over the duration of a typical storm event in our area (~48 h) and that it can be accurately characterized by the most up-to-date $SC_{pre\text{-}event}$ preceding an event. Second, changing the SC_{runoff} value from 5 to 100 μS cm^{-1} led to only 4 % deviation in the average contributions of runoff and baseflow, indicating variations in SC_{runoff} do not significantly impact our results as their magnitudes will be relatively small (< 100 μS cm^{-1}) compared to average stream SC_{total} (> 600 μS cm^{-1}). Lastly, we only analyze events characterized by dilution rather than mobilization ($FI < 0$) to ensure that our end-members are different, i.e., $SC_{runoff} < SC_{pre\text{-}event}$. In addition to SC-EMMA method, we also performed hydrograph separation using a Recursive Digital Filtering (RDF) to provide a second method of estimating runoff and baseflow components as a comparison to SC-EMMA. The RDF was performed using the HydRun package in MATLAB (Tang and Carey, 2017). All filtering parameters were set to their default values in the HydRun software. The primary output from the RDF is surface runoff, which is intended to represent overland flow, and baseflow, which we take to represent soil and groundwater contributions.

To determine the likely drivers of hydrologic pathways for each watershed, we compared a suite of hydroclimatological variables as potential event controls of Q_{runoff} and $Q_{baseflow}$. Previous research has indicated that the contribution of runoff to stormflow is largely influenced by both event characteristics and antecedent wetness (von Freyberg et al., 2018; Pellerin et al., 2008). High-intensity storms tend to saturate the soil more quickly, leading to an increase in runoff and a decrease in infiltration (Sherriff et al., 2016; Hamshaw et al., 2018). Additionally, while the impact of antecedent wetness on runoff contribution is more location-specific when compared to event characteristics, studies have suggested that wetter conditions generally result in smaller runoff contributions since the pre-event water available in subsurface layers can be rapidly activated by incoming precipitation (von Freyberg et al., 2018). Thus, we broadly classify these explanatory drivers as discharge, antecedent, or rainfall variables. Discharge variables are Q_{peak} (peak flow), I_{flood} (flood intensity), t_{storm} (storm duration), and t_{peak} (time-to-peak flow). Antecedent variables are Q_{base} (baseflow), AP_3 (three-day antecedent rainfall), AP_{14} (fourteen-day antecedent rainfall), and t_{gap} (time between events). Lastly, rainfall variables include P (precipitation), I_{30} (thirty-minute rainfall intensity), and t_{rain} (rainfall duration). The methodology for calculating each parameter is explained in a prior study within the same basins (Zarnaghsh and Husic, 2021). The fractional contribution of Q_{runoff} and $Q_{baseflow}$ for each event was compared to the suite of explanatory variables using Spearman rank correlation.

3.3. Runoff and baseflow contributions to sediment generation

To investigate the influence of runoff and baseflow pathways on suspended sediment generation during storm events, we employed constrained multiple linear regression (MLR) analysis to hydrograph separation results and high-frequency turbidity data (Fig. 3). For each qualifying event, we aimed to estimate whether the temporal structure of the observed turbidity time-series (T_{data}) aligned more closely with Q_{runoff} or $Q_{baseflow}$. To do this, we fit an MLR to each event, at the 15-min timestep, with Q_{runoff} and $Q_{baseflow}$ as the dependent variables. For each event, the MLR has the following form

$$T_{model} = \beta_{runoff}Q_{runoff} + \beta_{baseflow}Q_{baseflow} + \epsilon \quad (5)$$

where T_{model} is the modeled in-stream sediment concentration (mg/L), β_{runoff} and $\beta_{baseflow}$ are the runoff and baseflow slope coefficients, and ϵ is the error term. We constrain the regression so that β_{runoff} and $\beta_{baseflow}$ are always ≥ 0, i.e., they either contribute positively or not at all to sediment generation. We infer that the magnitudes of β_{runoff} and $\beta_{baseflow}$ suggest the relative importance of the respective flow components to overall sediment generation in the stream. This type of inference has shown recent utility in the literature, as in Nazari et al. (2021) for phosphorus transport in a tile-drained landscape. To assess the performance of the MLR to accurately simulate the suspended sediment time-series, we calculated the R^2 value for

each storm, and retain only events with an $R^2 > 0.70$ for further analysis. Ninety percent of events satisfy this criteria.

We introduce a normalized index (β'_{runoff}) that identifies the relative importance of the runoff pathway to riverine suspended sediment generation. The index can be calculated as

$$\beta'_{\text{runoff}} = \frac{\beta_{\text{runoff}}}{\beta_{\text{runoff}} + \beta_{\text{baseflow}}} \quad (6)$$

The index is normalized between 0 and 1, where a score of '0' indicates that the total suspended sediment time-series is entirely uncorrelated with timing or magnitude of runoff (Q_{runoff}). On the other hand, a score of '1' indicates that T_{model} is largely controlled by Q_{runoff} timing and magnitude. A storm event with equal contribution of Q_{runoff} and $Q_{baseflow}$ would have a β'_{runoff} of 0.5. We provide suggested ranges for β'_{runoff} of 0.0–0.3 for "Baseflow Control", 0.30–0.70 for "Pathway Balance", and 0.70–1.00 for "Runoff Control". We calculate β'_{runoff} for all qualifying events across our three basins to investigate if land use or storm event size impart influence on the relative importance of runoff to sediment generation.

4. Results

4.1. High-frequency sensing of solute dynamics and hysteresis

Across the twelve-year study period (2002 to 2014), a total of 864 storm events were identified, ranging from 177 in Rural Stream to 276 in Mixed Stream to 411 in Urban Stream (Fig. 4). Visual inspection of the discharge and *SC* time-series highlights contrasting event-scale patterns that vary

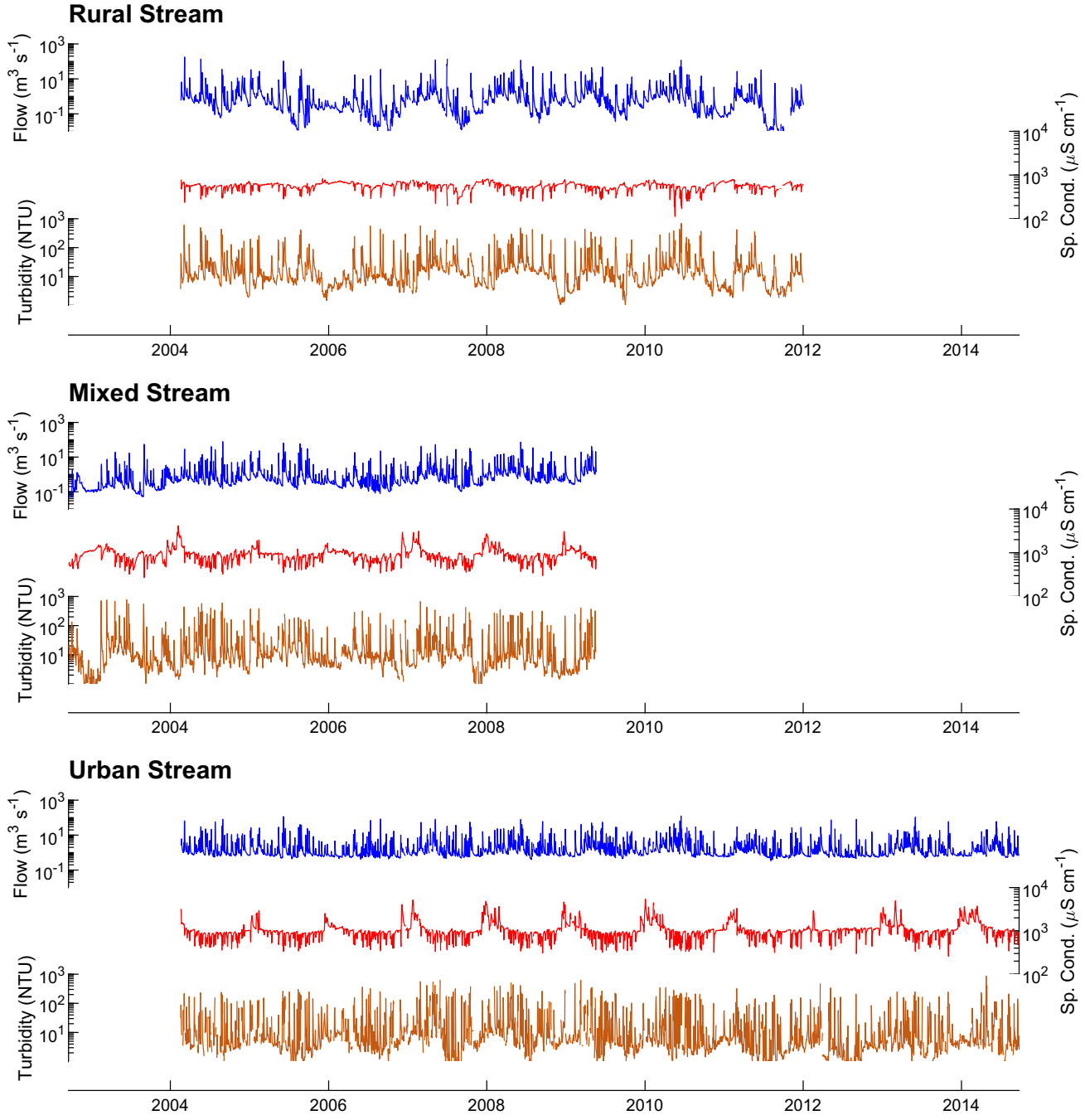

Fig. 4. Time-series of flow rate, specific conductance, and turbidity for the rural, mixed, and urban land use watersheds.

based on urban land use percentage. In Rural Stream, storm events are less flashy with an average time to peak flow of 14.0 h. The stream occasionally becomes very dry, and the in-stream *SC* typically has a consistent baseline value (median: 576 μS cm^{-1}), with dilution in response to events (minimum: 113 μS cm^{-1}). As we transition to the Mixed and Urban Streams, we observe flashier storm events with average time to peak flow of 8.4 and 6.1 h, respectively. The urban streams also trend toward higher baseflow values, which are sustained by one or multiple wastewater treatment facility discharges in each basin. Further, the baseline *SC* in Mixed Stream (884 μS cm^{-1}) and Urban Stream (968 μS cm^{-1}) are much greater than in Rural Stream. During dry periods, which are most evident each winter in Urban Stream, *SC* values can spike as high as 5385 μS cm^{-1} and likely consist entirely of wastewater effluent. The initiation of a storm event can occasionally cause a small flush of stored near-stream *SC* through the system that may later be drowned out by dilution, termed the 'first flush', which ranged from 51 to 80 μS cm^{-1} in our basins (Table S2). Approximately 20 % of Rural and Mixed Stream events experienced this flush while only 7 % of Urban Stream events did, likely due to the very high background wastewater effluent-driven *SC* in the Urban Stream.

Across all three basins, most storm events caused clockwise *SC* dilution (HI > 0 and FI < 0), suggesting that water with less *SC* arrives later in a hydrograph, either from distal locations or sources that are slowly mobilized (Fig. 5). A breakdown of events based on the timing of roadway brine application shows a shift in the in-stream flushing and hysteresis behavior, and that the manner of this shift depends on land use. In the Rural Stream, storms after brining ($n = 21$) have a significantly higher HI ($p < 0.05$) than non-brining events ($n = 156$) but exhibit no differences in FI ($p = 0.93$), suggesting the solute source is more proximal to the monitoring site but not necessarily more concentrated. In the Mixed Stream, events after brining ($n = 24$) have a significantly lower HI ($p < 0.05$) than non-brining events ($n = 252$) but exhibit no differences in FI ($p = 0.41$), suggesting more connectivity of distal solute sources in the mixed system than in the rural system. Lastly, in the Urban Stream, events after brining ($n = 41$) have a significantly lower HI ($p < 0.05$) than non-brining events ($n = 370$) as well as significantly higher FI ($p < 0.05$), indicating more intense distal flushing of solute than in the other two basins. For non-brining events in Urban Stream (Fig. S3), the vast majority (92 %) of events are characterized by clockwise-dilution of *SC*. This is largely because the baseflow *SC* is so large in Urban Stream – due to the multiple wastewater treatment facility operations in the basin – that any kind of event is likely to dilute the pre-existing baseflow *SC* values. However, for events following brine application, 66 % were characterized by flushing, likely because of the heavy brine application to the expansive and extensive impervious surfaces and roadway networks in the highly developed basin. With an understanding of *SC* dynamics of baseflow and runoff, in the next section we proceed to use these data to quantitatively separate total streamflow into its constituent components.

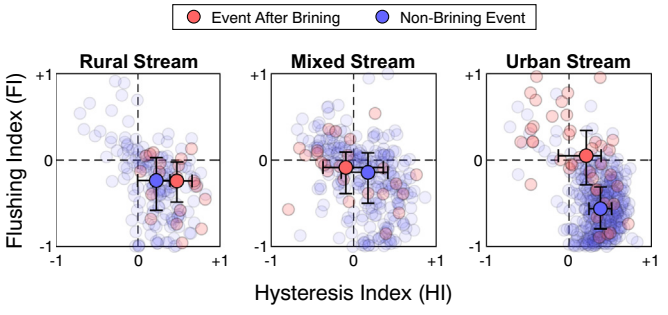

Fig. 5. Hysteresis and flushing indices for the study watersheds for non-brining storms and storms immediately following brining application. Solid markers represent the median values with 50 % prediction error bars. Transparent markers represent individual events.

4.2. Hydrograph separation of runoff and baseflow

Of the 864 total events, a subset of 222 events satisfied the SC-EMMA criteria for hydrograph separation (as explained in Section 3.2). The events include 38 in Rural Stream, 44 in Mixed Stream, and 140 in Urban Stream. To ensure that this smaller subset of storms was representative of all events, we compared the mean discharge of events that qualified for SC-EMMA (7.9 ± 6.1 $m^3 s^{-1}$) and those that did not (7.5 ± 15.9 $m^3 s^{-1}$), and we find no significant difference ($p = 0.77$ using a Mann-Whitney test). Regarding water components, all watersheds show the prominence of baseflow (plus wastewater effluent, if present) to the overall event discharge (Fig. 6). Importantly, as watersheds urbanize, the fraction of runoff to total streamflow increases from 0.31 ± 0.14 (Rural Stream) to 0.38 ± 0.15 (Mixed Stream) to 0.43 ± 0.14 (Urban Stream). In Mixed Stream, the single small wastewater treatment facility has negligible contribution to total streamflow (0.02 ± 0.01), whereas in the Urban Stream effluent from the two large facilities constitutes a significant fraction of streamflow (0.19 ± 0.11). Rural Stream does not contain a wastewater treatment facility thus its baseflow entirely consists of shallow subsurface and deeper groundwater flows. The inner quartile ranges of Q_{runoff}, $Q_{baseflow}$, and Q_{wwtf} predictions are somewhat wide because each individual event has unique climatological and antecedent drivers, causing variable hydrologic responses from one event to the next across basins. Table S3 shows the hydrograph separation results obtained using RDF. Although we observed a similar pattern in the variability of runoff and baseflow contributions across the three watersheds using both RDF and SC-EMMA, RDF showed slightly higher runoff contributions in all three watersheds. This difference may be due to the use of a filtering coefficient value that was not calibrated for our study watersheds.

Runoff and baseflow fractions to the overall storm event discharge were strongly related to the peak event discharge, Q_{peak} (Fig. 6). In all three streams, as Q_{peak} increases, the fractional contribution of Q_{runoff} increases while $Q_{baseflow}$ and Q_{wwtf} decrease. This effect is more prominent in the rural system compared to the mixed and urban streams. Spearman correlation (ρ) reinforced the importance of event and rainfall intensity as drivers of runoff fraction as Q_{peak}, flood intensity (I_{flood}), event precipitation (P), and thirty-minute rainfall intensity (I_{30}) were the most prominent hydroclimatological predictors (Table S4). The explanatory strength of these predictors typically reduced as basins urbanized, indicating added complexity of urbanization to runoff processes. For example, Q_{peak} correlation with Q_{runoff} decreased from the rural ($\rho = 0.89$) to mixed ($\rho = 0.78$) to urban ($\rho = 0.65$) systems. Likewise, P correlation with Q_{runoff} fraction followed a similar pattern from rural ($\rho = 0.70$) to mixed ($\rho = 0.65$) to urban ($\rho = 0.52$) systems. Predictors related to antecedent conditions (Q_{base}, AP_3, and AP_{14}) and timing (t_{storm}, t_{peak}, t_{gap}, and t_{rain}) were relatively uncorrelated with Q_{runoff} fraction and did not indicate behavior that systematically varies with land use.

4.3. Runoff and baseflow contributions to sediment generation

Of the 222 events that met the criteria for SC-EMMA analysis, 154 events also had concurrent turbidity data. Therefore, we performed our MLR analysis on these 154 events to develop a new index (β'_{runoff}) that identifies the relative importance of runoff and baseflow to stream suspended sediment (Fig. 7). As a reminder, a β'_{runoff} value of '1' indicates that the stream sediment signal has strong temporal alignment with Q_{runoff} whereas a value of '0' indicates the inverse, i.e., the sediment signal is strongly correlated with the timing of $Q_{baseflow}$. The MLR approach was successful in explaining the bulk of variance ($R^2 > 0.70$) in the sediment time series for 138 of 154 events, giving us confidence in the robustness of the approach.

To visually demonstrate the concept of β'_{runoff}, we present time series of total flow, baseflow, runoff, conductivity, and sediment concentration for three selected storms across a range of β'_{runoff} values (Fig. 7). Storm events where sediment arrival to the stream coincides with runoff are characterized by a larger β'_{runoff} value. In these "Runoff Control" type events,

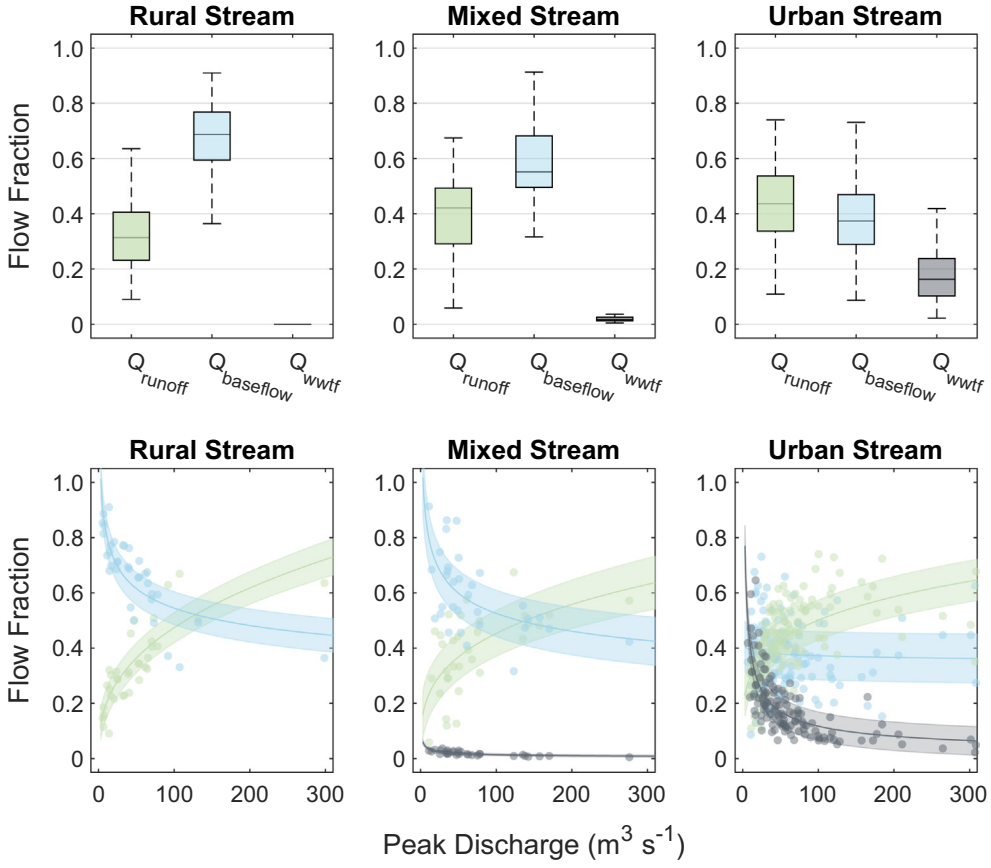

Fig. 6. Boxplots of fractional Q_{runoff}, $Q_{baseflow}$, and Q_{wwtf} contribution to stormflow (top row). Q_{runoff}, $Q_{baseflow}$, and Q_{wwtf} contribution results as a function of peak event discharge (bottom row). Power regressions are fit to each of the pathways (solid lines) and the 50 % prediction interval is plotted (shaded regions).

sediment concentration does not significantly increase until the contribution of Q_{runoff} is initiated. Further, the sediment concentration peak occurs almost simultaneously with the maximum value of Q_{runoff}. Hence, in this storm event, the sediment signal is predominantly influenced by runoff dynamics, even though runoff constitutes a smaller proportion of the total stormflow. When neither runoff or baseflow have an outsized influence, such as in the "Pathway Balance" event, multiple peaks in sediment concentration may correspond to pulses of sediment delivered by both the Q_{runoff}

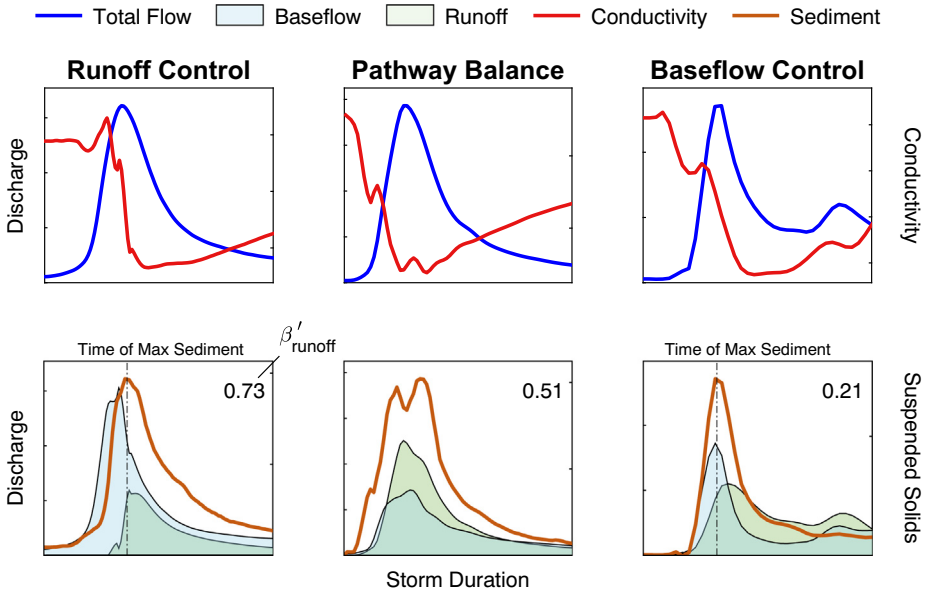

Fig. 7. Total flow, baseflow, runoff, conductivity, and suspended sediment for three selected storms along with their respective β'_{runoff} values. Events are ranked from left to right based on their β'_{runoff} value, from Runoff Control to Pathway Balance to Baseflow Control. Each plot is normalized by event duration and maximum discharge and sediment concentration.

and $Q_{baseflow}$ pathways. Finally, in "Baseflow Control" events, the observed sediment pattern is strongly correlated with the temporal structure of $Q_{baseflow}$ rather than Q_{runoff}. A rapid increase in sediment can be observed when the baseflow grows, followed by a dilution when baseflow begins to decrease. An important caveat to note is that a β'_{runoff} value of '1', for example, does not indicate that runoff is the only contributor of sediment to a stream, but rather that the in-stream sediment response is strongly aligned with the temporal structure of runoff arrival. Likewise, a β'_{runoff} value of '0' does not suggest that stream sediment is exclusively generated via baseflow. Nonetheless, understanding how sediment and hydrologic pathway signals coincide can be informative to understanding the response of a watershed to rain events.

Analysis of all storm events reveals mean β'_{runoff} values for Rural, Mixed, and Urban Streams to be 0.70, 0.57, and 0.64, respectively (Fig. 8). These results indicate a greater net impact of Q_{runoff} on the sediment concentration signal, i.e., $\beta'_{runoff} > 0.50$, for all three basins, but to varying extents. Notably, β'_{runoff} is greater in the Rural Stream than the basins experiencing substantial urbanization. To understand the hydroclimatological predictors of β'_{runoff}, we performed a correlation analysis that revealed a significant negative relationship between β'_{runoff} and Q_{peak}, I_{flood}, and P ($p < 0.01$), suggesting that storm size and intensity play a role in shifting the hydrologic pathways of sediment transport.

To varying degrees, β'_{runoff} results suggest a shift in the water pathways delivering high sediment concentrations, from Q_{runoff} sourcing at lower flows to $Q_{baseflow}$ sourcing at higher flows (Fig. 8). This was most true for the Rural Stream where the sediment signal for smaller events ($Q_{peak} < 20\ m^3\ s^{-1}$) is almost entirely controlled by the timing and magnitude of Q_{runoff} ($\beta'_{runoff} > 0.70$) whereas for larger events ($Q_{peak} > 20\ m^3\ s^{-1}$), the sediment signal shifts toward greater alignment with the timing and magnitude of $Q_{baseflow}$ ($\beta'_{runoff} < 0.30$). While this relationship is strong for Rural Stream ($R^2 = 0.73$), it begins to weaken under greater anthropogenic stresses in Mixed Stream ($R^2 = 0.59$) and Urban Stream ($R^2 = 0.09$). Unlike in Rural Stream, where sediment concentrations in small events was largely associated with runoff contribution, this was not always the case for the urbanized streams. In Urban Stream, two events with the same Q_{peak} can be characterized by vastly different β'_{runoff} values, suggesting entirely different hydrologic delivery pathways of sediment. The ability of hydroclimatological drivers to explain the behavior of β'_{runoff} weakens as basins urbanize, suggesting other non-hydroclimatological controls, such as the addition of impervious surfaces or the removal of riparian buffers.

5. Discussion

We performed hysteresis analysis, hydrograph separation, and multiple linear regression on hundreds of events to gain better insight into how land use affects solute dynamics and the generation of high-sediment water by runoff and baseflow pathways. Our results showed solutes are generally source-limited; however, winter brining in the urban watershed led to a significantly increased distal connectivity of solutes. These results emphasize the role of urbanization in augmenting the hydrologic connectivity of a basin. Regarding sediment, multiple linear regression results between in-stream total suspended sediment and hydrologic pathways showed overall alignment of sediment with runoff, but also that baseflow becomes more relevant to sediment generation in urbanized watersheds and during large storms. These results support our initial hypothesis of the augmented role of subsurface flow in eroding, transporting, and delivering sediment to urbanized streams.

5.1. Urbanization increases the connectivity of distal salty runoff to the streams

While it is well-established that urbanization accelerates the trend of freshwater salinization, largely due to the excess application of road deicers (Moore et al., 2020; Kaushal et al., 2021), our knowledge regarding how anthropogenic disturbances change the sourcing and transport dynamics of solutes during storm events is less certain. We found one paper in the literature that employs high-frequency data to analyze the impact of road salt application to salinity hysteresis patterns (Lakoba et al., 2020). In that study, the authors reported no clear change in river flushing or hysteresis behavior in response to brine application for 114 events in a single mixed-use watershed. To extend this analysis, we calculated the same metrics for 864 events, occurring over twelve years, in three basins along an urbanization gradient. This analysis helped us answer the following questions: 1) how do urban elements affect the connectivity of solutes to streams in the presence and absence of road salts, and 2) how anthropogenic activities such as wastewater effluent impact the flushing and diluting patterns of salt during storm events?

For non-brining events, the dominant SC hysteresis type was diluting-clockwise in all watersheds regardless of land use (Fig. S3), indicating solutes are primarily stored in the near-channel riparian zones and that they are rapidly depleted upon storm onset (Wymore et al., 2019; Miller et al., 2021). The independence of geogenic solute transport to land use and hydroclimatic conditions has previously been observed in forested and agricultural settings (Musolff et al., 2021; Koenig et al., 2017). Here, we observe the same patterns for urban watersheds, indicating the spatial and temporal homogeneity of solutes in the absence of brine application. The diluting impact of storm event on groundwater-sourced solutes was most evident in Urban Stream, where wastewater treatment facility discharge constitutes an average of 80 % flow during extended baseflow periods (Zarnaghsh and Husic, 2021), thereby seeding the stream with very high salinity water prior to storm onset. After rainfall, urban features, such as storm sewers and drainage ditches, rapidly transfer less salty runoff to streams, resulting in the observed diluting pattern. Due to the high antecedent salinity in the Urban Stream, it had half as many 'first flush' events as the Mixed and Rural Streams (Table S2) likely because the near-stream salt stores that are initially flushed are less concentrated than the existing in-stream wastewater effluent. These results emphasize the impact wastewater treatment facilities have on in-stream salt levels even in the absence of road deicing operations.

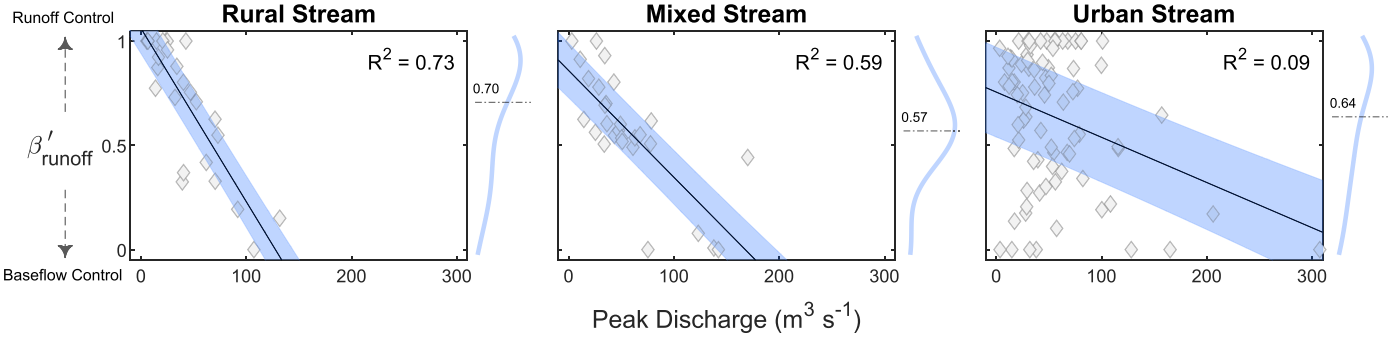

Fig. 8. β'_{runoff} vs peak discharge for all storms. Linear regressions are fit to each of the streams (solid lines) and the 50 % prediction interval for each regression is plotted (shaded regions). A kernel density distribution of β'_{runoff} for each basin is plotted to the right of each tile. The median of the β'_{runoff} distribution for each basin is indicated by a dashed line and text.

For events immediately following brine application, we observed different *SC* hysteresis based on land use. In the rural watershed, where the amount of salts applied is expected to be lower given the smaller roadway density (Table S1), the dominant hysteresis remained diluting with no counterclockwise events identified (Fig. S3), suggesting that whatever road salts were applied did not have the necessary hydrologic connectivity to arrive to the monitoring location, potentially due to the presence of disconnecting features such as vegetation and flow limitation (Lakoba et al., 2020). In contrast, the Urban Stream was characterized by a significant increase in the proportion of flushing events and counterclockwise hysteresis patterns, indicating not only widespread availability of road salts, but also the necessary connectivity to the fluvial network. The removal of vegetation and the channelization of flow paths through drainage ditches likely accelerates solute delivery, as has been noted for sediment delivery in prior study of these basins (Zarnaghsh and Husic, 2021). As a result, artificial pathways such as storm drainage systems have the potential to become primary methods of salt transport to urban streams.

Together, our finding shows urbanization can have a dual impact on solute transport dynamics. During the non-winter period when distal salt availability is limited, direct delivery of runoff by impervious surfaces and storm drainage networks dilutes the salty baseflow in urban streams (Long et al., 2017). However, when brine is applied to the roadway, the same connectivity mechanism is responsible for the direct mobilization of road salts, as evidenced by a 50 % increase in flushing behavior in the Urban Stream. Therefore, flushing of salt to streams due to the application of road-brine can be reduced by utilizing storm drainage mechanisms such as detention ponds that delay the delivery of solutes to fluvial systems. (Daley et al., 2009; Long et al., 2015). Analyzing the solute-discharge relationship across an urbanization gradient revealed that the relationship between proportion of flushing events in a basin is not linearly related to fraction of impervious surfaces. In other words, mixed-use watersheds may not necessarily flush solutes following road salt application – even given a large fraction of urban land use (62 % in our Mixed Stream; Table S1). However, at some point, a threshold is reached whereby the amount of urbanization is considerable enough to overcome disconnectivities in the system and the stream behavior shifts toward flushing in response to most brining events. Lakoba et al. (2020) attributed this behavior to watershed complexity caused by multiple transport mechanisms (e.g., drainage systems, impoundments, etc.) and salt inputs (e.g. agricultural inputs) in mixed streams (Lakoba et al., 2020). We observed similar complexity and variability in the Mixed Stream. However, in the Urban Stream, there was a clear difference in *HI* and *FI* between brining and non-brining events, suggesting that once the degree of urbanization exceeds a certain point, urban features simplify complexities related to solute dynamics and make the impact of brining on flushing and diluting behavior clearer.

5.2. Urbanization adds complexity to sediment delivery pathways during storm events

Despite the important role urbanization plays in accelerating streambank erosion (Whitney et al., 2015; Pickering and Ford, 2021; Percich et al., 2022), the specific pathways of water that are responsible for eroding and transporting this bank material are not as well understood. In this study, we develop and apply a new index – β'_{runoff} – to quantitatively compare the relative significance of surface runoff and subsurface baseflow to the temporal structure of sediment generation. Prior sediment tracing work in our three study basins, using plutonium isotopes (Percich et al., 2022), showed that the fraction of sediment originating from subsurface bank sediment was 50 % in the Rural Stream and 93 % in the Urban Stream. While we understand the source of suspended sediment in our basins, it is uncertain what hydrologic pathway cause its erosion and transport, a challenge often posed in urban water quality work (Oswald et al., 2023). Thus, in this study, we answer the following questions: 1) is the timing of in-stream sediment generation correlated more strongly with runoff or baseflow, and 2) how does urbanization alter the correlation of sediment generation with runoff and baseflow?

Our hydrograph separation results showed faster mobilization of "old" water – as opposed to "new" runoff – during the rising limb of the majority (58 %) of storm events, which is known as the "old water" paradox. The paradoxical rapid mobilization of old water in urban watersheds remains an open question, despite well-known surface runoff pathways such as impervious channels and roadway drainage ditches. Researchers attribute this rapid delivery of pre-event water to mechanisms such as the mobilization of high-conductivity soil water and lateral flow at the soil-rock interface (Bhaskar and Welty, 2015). Others, such as Yang et al. (2021) and Pellerin et al. (2008), suggest that this water component may represent water flushed from swamps and depressions or flood-waves of baseflow water displaced by runoff, rather than the slow bank storage return flow that typically emerges during the falling limb of storm events. Our results lead us to support the former hypothesis whereby storm events rapidly flush out water stored in near-channel soil zones in a piston-like manner, as supported by the work of Bhaskar and Welty (2015) and Bonneau et al. (2018). This flushing of "old" water occurs prior to the arrival of surficial runoff and is accompanied by an increase in sediment concentrations as the arriving subsurface water entrains readily erodible sediment from recent streambed deposits or exposed banks.

The mean value of β'_{runoff} was larger than 0.5 for all watersheds, regardless of land use, suggesting that, whatever the mechanism of the rapid mobilization of old water is, the dynamics of in-stream suspended sediment are more aligned with surface runoff than baseflow. Thus, despite the rapid arrival of old water to the stream and its generation of a sediment pulse, much of the overall storm sediment delivery occurs because of runoff arrival. This is consistent with previous studies that have shown the important role of surface runoff in erosion and delivery of sediments to water bodies (Da Silva et al., 2013; Boithias et al., 2021). Interestingly, the mean β'_{runoff} was slightly smaller in the mixed ($\beta'_{runoff} = 0.57$) and urban ($\beta'_{runoff} = 0.64$) streams compared to rural stream ($\beta'_{runoff} = 0.70$), indicating an elevated role of baseflow in suspended sediment generation in the urban basins, potentially due to the limited upland sediment availability caused by the presence of impervious surfaces (Mahoney et al., 2021).

While the mean β'_{runoff} was generally similar across the three sites, how β'_{runoff} varied as a function of maximum event discharge was considerably different between the Rural and Urban Streams. In Rural Stream, we observed a negative correlation between storm peak flow and β'_{runoff} ($R^2 = 0.73$; Fig. 8), suggesting that suspended sediment generation becomes more aligned with the mobilization of old water to the streams during more intense storm events. This is particularly interesting because our correlation analysis indicated that larger events are characterized by a smaller baseflow fraction of storm flow (Table S4). During small events, water stored in the unsaturated zone is less hydrologically connected to streams, and thus the majority of sediments are delivered by runoff arrival. However, as storm events become more intense, subsurface pathways become more activated, enabling erosive water to be quickly transported to streams during the rising limb (Nazari et al., 2021; Sherriff et al., 2019; Bieroza and Heathwaite, 2015). This rapid mobilization of water stored in the unsaturated zone, coupled with flow from well-drained soils, generates considerable shear forces that are capable of eroding streambank materials (Oeurng et al., 2010; Sherriff et al., 2019), and creating the large early peak in sediment concentration we often observed (Fig. 8). As the storm event progresses, although runoff continues to be transported to the stream, it carries less and less sediment due to the depletion of upland sources. This results in a larger contribution of runoff to storm flow, but a larger contribution of base flow to suspended sediment generation. Previous studies, including a study on the same watershed, have shown that larger peak flow promotes a clockwise turbidity hysteresis pattern, suggesting a more significant proximal sourcing (Zarnaghsh and Husic, 2021; Hamshaw et al., 2018). Our hydrograph separation results indicate that this larger fraction of clockwise pattern is most likely due to the increased transport of sediment caused by the delivery of water from subsurface pathways rather than surface runoff.

In contrast to the Rural Stream, very little correlation was observed between β'_{runoff} and peak discharge in the Urban Stream ($R^2 = 0.09$; Fig. 8), indicating a more complex relationship between the timing of water components and suspended sediment in developed streams. Previous studies have attributed the temporal variability in sediment-discharge relationship to the activation of multiple sources, including in-channel/gully erosion, resuspension of recently deposited sediment in the fluvial network, and construction sites and road networks (Pickering and Ford, 2021; Gellis and Noe, 2013). However, our sediment tracing study in the urban site indicated that the source of transported material is always the same, with 93 % of suspended sediment originating as bank material in the Urban Stream (Percich et al., 2022). Therefore, we argue that the variability in response mostly originates from the variability in hydrological pathways by which pre-event and runoff water components are transported to the channels and lead to the erosion of bank material, which is already facilitated by the removal of riparian vegetation and wastewater contributions. While numerous previous studies have shown large fraction of pre-event water contributions to stormflow in urban watersheds (Bhaskar and Welty, 2015; Pellerin et al., 2008), we show in this study that this mobilization of pre-event water corresponds to an increase in suspended sediment.

Urban features add complexity and variability to the hydrologic pathways that transport sediment to the stream network, which we try to understand through analysis of event-based variables. We considered a slew of discharge (Q_{peak}, I_{flood}, t_{storm}, and t_{peak}), antecedent (Q_{base}, AP_3, AP_{14}, and t_{gap}), and rainfall (P, I_{30}, and t_{rain}) variables to try to explain the behavior of β'_{runoff} as landscapes urbanize, but the variables provided limited explanatory strength. This is in line with the results of a previous study that showed that the flashier an urban stream, the more difficult its sediment response is to predict solely using discharge (Chen and Chang, 2019). Thus, we believe that observed variability of β'_{runoff} is a result of land use differences and the arrangement of urban features as opposed to hydroclimatological processes. First, impervious surfaces blanket and disconnect upland sediment that would otherwise have the potential for erosion and transport to the stream corridor (Devereux et al., 2010; Russell et al., 2019). Second, because of the lack of upland erosion to satisfy the sediment transport carrying capacity of runoff, impervious surfaces, wastewater treatment facilities, and drainage networks convey relatively sediment-free (or 'hungry') water into stream networks where it can rapidly erode bank material (Heckmann et al., 2017; Russell et al., 2020). These features likely play a large role in modifying the pathways of sediment delivery in urban systems, while ultimately causing the same type of sediment to be eroded, i.e., bank material. Together, our findings suggest that constraining excess bank erosion in urban basins must consider not only surficial runoff, which is often the prime focus for management, but also subsurface baseflow, which we show to be relatively more important to sediment generation in urban than rural streams.

5.3. An index for identifying hydrologic pathway influence on water quality

In this study, we couple hydrograph separation with high-frequency sensing of sediment to develop a quantitative index – β'_{runoff} – to gain a better understanding of sediment generation in rivers. This index quantifies the relative contribution of runoff and baseflow to the temporal structure of in-stream sediment. Beyond our development of β'_{runoff} for turbidity data, there is clear potential for its application to other aquatic sensing data sets, including nitrate, phosphorus, dissolved organic matter, and chlorophyll-a, to name a few, so long as coincident specific conductance data (or other methods) are available for hydrograph separation. For example, applying β'_{runoff} to nitrate data would improve understanding of the flow pathways associated with nitrate arrival to the stream network, which is a major challenge for effective management of non-point source pollution. Nazari et al. (2021) use multiple linear regression to assess phosphorus transport in a tile-drained landscape, which could be expanded, as in our study, to consider the temporal coherence of phosphorus stores and hydrologic pathways. Studies in the literature stress the importance that timing prediction plays in the success of measures aimed at reducing problems caused by sediment erosion and other pollutant-generating events (Zaimes et al., 2021; Mohanavelu et al., 2022).

Despite the utility of β'_{runoff}, there are several considerations that need to be made prior to its use. First, it is important to note that β'_{runoff} does not quantify the magnitude of the sediment yield carried by a hydrologic pathway, but rather represents the temporal correlation between the arrival of a hydrologic pathway to the stream and the corresponding response of the sediment signal – a slight but important distinction. Quantifying sediment loading due to each component would require detailed knowledge of the sediment source end-member concentrations, which may not be stationary through time and thus would violate mixing model assumptions. Second the values we get from β'_{runoff} are heavily dependent on the method of hydrograph separation (EMMA vs RDF). We recommend SC-EMMA as it provides a flow-independent approach that is unique to each storm event and not influenced by the selection of filtering parameters. Digital filter methods, by their mathematical construction, impose that baseflow arrives after runoff, which may not be the case in many basins. Because we use linear regression in calculating β'_{runoff}, the model may not entirely capture nonlinear relationships that exist in the data, and it may be sensitive to outliers and noise in the turbidity signal. Nonetheless, β'_{runoff} was shown in this study to be a robust tool for the assessment of hydrologic pathway influence to sediment generation across 138 events, and it has potential promise for application to other high-frequency aquatic sensing data sets.

6. Conclusions

The rapidly increasing availability of high temporal resolution water quality data provides a great opportunity to assess the impact of land use change on hydrologic pathways and sediment transport. Analyzing over a decade of specific conductance data in three watersheds along a rural-to-urban transect, we found that urbanized streams are significantly more prone to salinization due to the enhanced hydrologic connectivity of deicing agents distal to the stream network. Hydrograph separation results showed an increasing fractional contribution of runoff to total streamflow as a function of land use: rural stream (0.31 ± 0.14), mixed stream (0.38 ± 0.15), urban stream (0.43 ± 0.14). Turbidity data and hydrologic pathway results were coupled to create a new quantity index describing the temporal structure of sediment delivery to streams, β'_{runoff}. In the rural basin, in-stream sediment is strongly correlated to the arrival of runoff at low flows and to baseflow at high flows. Baseflow becomes more relevant to sediment generation in the most urban stream, potentially arising from relatively sediment-free runoff from impervious surfaces coupled with baseflow-driven erosion of streambanks. The new index developed as part of this study – β'_{runoff} – shows promise for identifying important hydrologic pathways to sediment generation as well as potential application to other water quality constituents, such as nitrate.

CRediT authorship contribution statement

A. Zarnaghsh: Conceptualization, Investigation, Methodology, Software, Data curation, Formal analysis, Visualization, Writing – original draft, Writing – review & editing. **A. Husic:** Conceptualization, Investigation, Methodology, Software, Data curation, Formal analysis, Visualization, Writing – original draft, Writing – review & editing.

Data availability

A link to the data repository where the data are stored is included in the Acknowledgements.

Declaration of competing interest

The authors declare that they have no known competing financial interests or personal relationships that could have appeared to influence the work reported in this paper.

Acknowledgments

The authors would like to thank Associate Editor Wei Ouyang and two anonymous reviewers for their constructive comments that helped improve the quality of this manuscript. Further, the authors thank the University of Kansas Department of Civil, Environmental, and Architectural Engineering for providing partial funding to the lead student author of this manuscript. The authors gratefully acknowledge Teresa Rasmussen of the USGS Kansas Water Science Center for providing knowledge of the study region and high-frequency sensor data used in this project. Modeling code, high-frequency sensor data, and model outputs are publicly available on Open Science Framework (at: https://doi.org/10.17605/OSF.IO/724KG). The authors have no conflicts of interest to declare.

Appendix A. Supplementary data

Supplementary data to this article can be found online at https://doi.org/10.1016/j.scitotenv.2023.164931.

References

Aguilera, R., Melack, J.M., 2018. Concentration-discharge responses to storm events in coastal California watersheds. Water Resour. Res. 54, 407–424. https://doi.org/10.1002/2017WR021578.

Bettencourt, L., Clarens, A., Das, S., Fitzgerald, G., Irwin, E., Pataki, D., Pincetl, S., Seto, K., Waddell, P., Nichols, L.G., 2018. Sustainable Urban Systems: Articulating a Long-Term Convergence Research Agenda. Washington, DC.

Bhaskar, A.S., Welty, C., 2015. Analysis of subsurface storage and streamflow generation in urban watersheds. Water Resour. Res. 51 (3), 1493–1513.

Bieroza, M.Z., Heathwaite, A.L., 2015. Seasonal variation in phosphorus concentration–discharge hysteresis inferred from high-frequency in situ monitoring. J. Hydrol. 524, 333–347.

Boithias, L., Ribolzi, O., Lacombe, G., Thammahacksa, C., Silvera, N., Latsachack, K., ... Rochelle-Newall, E., 2021. Quantifying the effect of overland flow on Escherichia coli pulses during floods: use of a tracer-based approach in an erosion-prone tropical catchment. J. Hydrol. 594, 125935.

Bonneau, J., Burns, M.J., Fletcher, T.D., Witt, R., Drysdale, R.N., Costelloe, J.F., 2018. The impact of urbanization on subsurface flow paths–a paired-catchment isotopic study. J. Hydrol. 561, 413–426.

Burns, D.A., Pellerin, B.A., Miller, M.P., Capel, P.D., Tesoriero, A.J., Duncan, J.M., 2019. Monitoring the riverine pulse: applying high-frequency nitrate data to advance integrative understanding of biogeochemical and hydrological processes. Wiley Interdiscip. Rev. Water e1348. https://doi.org/10.1002/wat2.1348.

Cartwright, I., Miller, M.P., 2021. Temporal and spatial variations in river specific conductivity: implications for understanding sources of river water and hydrograph separations. J. Hydrol. 593, 125895. https://doi.org/10.1016/j.jhydrol.2020.125895.

Cashman, M.J., Gellis, A., Sanisaca, L.G., Noe, G.B., Cogliandro, V., Baker, A., 2018. Bank-derived material dominates fluvial sediment in a suburban Chesapeake Bay watershed. River Res. Appl. 34, 1032–1044. https://doi.org/10.1002/rra.3325.

Chapman, J.M., Proulx, C.L., Veilleux, M.A.N., Levert, C., Bliss, S., André, M.È., Lapointe, N.W.R., Cooke, S.J., 2014. Clear as mud: a meta-analysis on the effects of sedimentation on freshwater fish and the effectiveness of sediment-control measures. Water Res. 56, 190–202. https://doi.org/10.1016/j.watres.2014.02.047.

Chen, J., Chang, H., 2019. Dynamics of wet-season turbidity in relation to precipitation, discharge, and land cover in three urbanizing watersheds, Oregon. River Res. Appl. 35, 892–904. https://doi.org/10.1002/rra.3487.

Da Silva, R.M., Santos, C.A.G., de Lima Silva, V.C., e Silva, L. P., 2013. Erosivity, surface runoff, and soil erosion estimation using GIS-coupled runoff–erosion model in the Mamuaba catchment, Brazil. Environ. Monit. Assess. 185, 8977–8990.

Daley, M.L., Potter, J.D., McDowell, W.H., 2009. Salinization of urbanizing New Hampshire streams and groundwater: effects of road salt and hydrologic variability. J. North Am. Benthol. Soc. 28, 929–940. https://doi.org/10.1899/09-052.1.

Demers, D.J., Green, M.B., Bailey, S.W., 2021. Semi-automated characterization of streamwater specific conductivity response to storms. J. Am. Water Resour. Assoc. https://doi.org/10.1111/1752-1688.12941.

Devereux, O.H., Prestegaard, K.L., Needelman, B.A., Gellis, A.C., 2010. Suspended-sediment sources in an urban watershed, Northeast Branch Anacostia River, Maryland. Hydrol. Process. 24, 1391–1403. https://doi.org/10.1002/hyp.7604.

Fitzpatrick, M.L., Long, D.T., Pijanowski, B.C., 2007. Exploring the effects of urban and agricultural land use on surface water chemistry, across a regional watershed, using multivariate statistics. Appl. Geochem. 22, 1825–1840. https://doi.org/10.1016/j.apgeochem.2007.03.047.

Fovet, O., Humbert, G., Dupas, R., Gascuel-Odoux, C., Gruau, G., Jaffrezic, A., Thelusma, G., Faucheux, M., Gilliet, N., Hamon, Y., Grimaldi, C., 2018. Seasonal variability of stream water quality response to storm events captured using high-frequency and multiparameter data. J. Hydrol. 559, 282–293. https://doi.org/10.1016/j.jhydrol.2018.02.040.

von Freyberg, J., Studer, B., Rinderer, M., Kirchner, J.W., 2018. Studying catchment storm response using event-and pre-event-water volumes as fractions of precipitation rather than discharge. Hydrol. Earth Syst. Sci. 22 (11), 5847–5865.

Gao, P., Josefson, M., 2012. Event-based suspended sediment dynamics in a Central New York watershed. Geomorphology 139, 425–437.

Gellis, A.C., Noe, G.B., 2013. Sediment source analysis in the Linganore Creek watershed, Maryland, USA, using the sediment fingerprinting approach: 2008 to 2010. J. Soils Sediments 13, 1735–1753.

Hamshaw, S.D., Dewoolkar, M.M., Schroth, A.W., Wemple, B.C., Rizzo, D.M., 2018. A new machine-learning approach for classifying hysteresis in suspended-sediment discharge relationships using high-frequency monitoring data. Water Resour. Res. 54, 4040–4058. https://doi.org/10.1029/2017WR022238.

Heckmann, T., Haas, F., Abel, J., Rimböck, A., Becht, M., 2017. Feeding the hungry river: fluvial morphodynamics and the entrainment of artificially inserted sediment at the dammed river Isar, Eastern Alps, Germany. Geomorphology 291, 128–142. https://doi.org/10.1016/j.geomorph.2017.01.025.

Iglesias, M.C.A., 2020. A review of recent advances and future challenges in freshwater salinization. Limnetica 39, 185–211. https://doi.org/10.23818/limn.39.13.

Kaushal, S.S., Likens, G.E., Pace, M.L., Utz, R.M., Haq, S., Gorman, J., Grese, M., 2018. Freshwater salinization syndrome on a continental scale. Proc. Natl. Acad. Sci. 115, E574–E583. https://doi.org/10.1073/pnas.1711234115.

Kaushal, S.S., Likens, G.E., Pace, M.L., et al., 2021. Freshwater Salinization Syndrome: From Emerging Global Problem to Managing Risks.

Koenig, L.E., Shattuck, M.D., Snyder, L.E., Potter, J.D., McDowell, W.H., 2017. Deconstructing the effects of flow on DOC, nitrate, and major ion interactions using a high-frequency aquatic sensor network. Water Resour. Res. 53, 10655–10673. https://doi.org/10.1002/2017WR020739.

Lakoba, V., Wind, L., DeVilbiss, S., Lofton, M., Bretz, K., Weinheimer, A., Moore, C., Baciocco, C., Hotchkiss, E., Hession, W.C., 2020. Salt Dilution and Flushing Dynamics of an Impaired Agricultural–Urban Stream. ACS ES&T Water. https://doi.org/10.1021/acsestwater.0c00160.

Lawler, D.M., Petts, G.E., Foster, I.D.L., Harper, S., 2006. Turbidity dynamics during spring storm events in an urban headwater river system: The Upper Tame, West Midlands, UK. Sci. Total Environ. 360, 109–126. https://doi.org/10.1016/j.scitotenv.2005.08.032.

Ledford, S.H., Toran, L., 2019. Downstream evolution of wastewater treatment plant nutrient signals using high-temporal monitoring. Hydrol. Process. 1–13. https://doi.org/10.1002/hyp.13640.

Lee, C., Rasmussen, P., Ziegler, A., Fuller, C., 2009. Transport and Sources of Suspended Sediment in the Mill Creek Watershed, Johnson County, Northeast Kansas, 2006-07. U.S. Geological Survey, pp. 2009–5001 SIR.

Liu, W., Youssef, M.A., Birgand, F.P., Chescheir, G.M., Tian, S., Maxwell, B.M., 2020. Processes and mechanisms controlling nitrate dynamics in an artificially drained field: insights from high-frequency water quality measurements. Agric. Water Manag. 232, 106032.

Lloyd, C.E., Freer, J.E., Johnes, P.J., Collins, A.L., 2016a. Technical note: testing an improved index for analysing storm discharge-concentration hysteresis. Hydrol. Earth Syst. Sci. 20, 625–632. https://doi.org/10.5194/hess-20-625-2016.

Lloyd, C.E., Freer, J.E., Johnes, P.J., Collins, A.L., 2016b. Using hysteresis analysis of high-resolution water quality monitoring data, including uncertainty, to infer controls on nutrient and sediment transfer in catchments. Sci. Total Environ. 543, 388–404. https://doi.org/10.1016/j.scitotenv.2015.11.028.

Long, D.T., Voice, T.C., Chen, A., Xing, F., Li, S.G., 2015. Temporal and spatial patterns of Cl- and Na+ concentrations and Cl/Na ratios in salted urban watershed. Elementa 3, 1–14. https://doi.org/10.12952/journal.elementa.000049.

Long, D.T., Voice, T.C., Xagaroraki, I., Chen, A., Wu, H., Lee, E., Oun, A., Xing, F., 2017. Patterns of c-q Hysteresis Loops and Within an Integrative Pollutograph for Selected Inorganic and Organic.

Mahoney, D., Blandford, B., Fox, J., 2021. Coupling the probability of connectivity and RUSLE reveals pathways of sediment transport and soil loss rates for forest and reclaimed mine landscapes. J. Hydrol. 594, 125963.

Michalek, A., Zarnaghsh, A., Husic, A., 2021. Modeling linkages between erosion and connectivity in an urbanizing landscape. Sci. Total Environ. 764, 144255. https://doi.org/10.1016/j.scitotenv.2020.144255.

Miller, M.P., Susong, D.D., Shope, C.L., Heilweil, V.M., Stolp, B.J., 2014. Continuous estimation of baseflow in snowmelt-dominated streams and rivers in the Upper Colorado River Basin: a chemical hydrograph separation approach Matthew. Water Resour. Res. 50, 6986–6999. https://doi.org/10.1002/2013WR014939.Received.

Miller, M.P., Tesoriero, A.J., Hood, K., Terziotti, S., Wolock, D.M., 2017. Estimating discharge and nonpoint source nitrate loading to streams from three end-member pathways using high-frequency water quality data. Water Resour. Res. 53, 10201–10216. https://doi.org/10.1002/2017WR021654.

Miller, A., Dere, A., Coleman, T., 2021. High-frequency data reveal differential dissolved and suspended solids behavior from a mixed restored prairie and agricultural catchment. Sci. Total Environ. 753, 141731. https://doi.org/10.1016/j.scitotenv.2020.141731.

Mohanavelu, A., Shrivastava, S., Naganna, S.R., 2022. Streambed pollution: a comprehensive review of its sources, eco-hydro-geo-chemical impacts, assessment, and mitigation strategies. Chemosphere 300, 134589. https://doi.org/10.1016/j.chemosphere.2022.134589.

Moore, J., Fanelli, R.M., Sekellick, A.J., 2020. High-frequency data reveal deicing salts drive elevated specific conductance and chloride along with pervasive and frequent exceedances of the U.S. Environmental Protection Agency aquatic life criteria for chloride in urban streams. Environ. Sci. Technol. 54, 778–789. https://doi.org/10.1021/acs.est.9b04316.

Musolff, A., Zhan, Q., Dupas, R., Minaudo, C., Fleckenstein, J.H., Rode, M., Dehaspe, J., Rinke, K., 2021. Spatial and temporal variability in concentration-discharge relationships at the event scale. Water Resour. Res. 57, 1–21. https://doi.org/10.1029/2020WR029442.

Namugize, J.N., Jewitt, G., Graham, M., 2018. Effects of land use and land cover changes on water quality in the uMngeni river catchment, South Africa. Phys. Chem. Earth 105, 247–264. https://doi.org/10.1016/j.pce.2018.03.013.

Nazari, S., Ford, W.I., King, K.W., 2021. Quantifying hydrologic pathway and source connectivity dynamics in tile drainage: implications for phosphorus concentrations. Vadose Zo J. https://doi.org/10.1002/vzj2.20154.

Oeurng, C., Sauvage, S., Sánchez-Pérez, J.M., 2010. Dynamics of suspended sediment transport and yield in a large agricultural catchment, Southwest France. Earth Surf Process Landforms 35, 1289–1301. https://doi.org/10.1002/esp.1971.

Oswald, C.J., Kelleher, C., Ledford, S.H., Hopkins, K.G., Sytsma, A., Tetzlaff, D., Toran, L., Voter, C., 2023. Integrating urban water fluxes and moving beyond impervious surface cover: a review. J. Hydrol. 618, 129188. https://doi.org/10.1016/j.jhydrol.2023.129188.

Pellerin, B., Wollheim, W., Feng, X., Vörösmarty, C., 2008. The application of electrical conductivity as a tracer for hydrograph separation in urban catchments. Hydro. Process. 22 (12), 1810–1818.

Percich, A., Husic, A., Ketterer, M.E., 2022. Plutonium isotopes: an effective tool for fluvial sediment sourcing in urbanized catchments. Geophys. Res. Lett. 49. https://doi.org/10.1029/2021GL094497 (e2021GL094497).

Pickering, C., Ford, W.I., 2021. Effect of watershed disturbance and river-tributary confluences on watershed sedimentation dynamics in the Western Allegheny Plateau. J. Hydrol. 602, 126784. https://doi.org/10.1016/j.jhydrol.2021.126784.

Rahmani, V., Kastens, J.H., de Noyelles, F., Jakubauskas, M.E., Martinko, E.A., Huggins, D.H., Gnau, C., Liechti, P.M., Campbell, S.W., Callihan, R.A., Blackwood, A.J., 2018. Examining storage capacity loss and sedimentation rate of large reservoirs in the Central U.S. great plains. Water 10, 1–17. https://doi.org/10.3390/w10020190.

Rasmussen, T., Gatotho, J., 2014. Water-Quality Variability and Constituent Transport and Processes in Streams of Johnson County, Kansas, Using Continuous Monitoring and Regression Models, 2003–11. Reston, VA.

Rode, M., Wade, A.J., Cohen, M.J., Hensley, R.T., Bowes, M.J., Kirchner, J.W., Arhonditsis, G.B., Jordan, P., Kronvang, B., Halliday, S.J., Skeffington, R.A., Rozemeijer, J.C., Aubert, A.H., Rinke, K., Jomaa, S., 2016. Sensors in the stream: the high-frequency wave of the present. Environ. Sci. Technol. 50, 10297–10307. https://doi.org/10.1021/acs.est.6b02155.

Russell, K.L., Vietz, G.J., Fletcher, T.D., 2018. Urban catchment runoff increases bedload sediment yield and particle size in stream channels. Anthropocene 23, 53–66. https://doi.org/10.1016/j.ancene.2018.09.001.

Russell, K.L., Vietz, G.J., Fletcher, T.D., 2019. Urban sediment supply to streams from hillslope sources. Sci. Total Environ. 653, 684–697. https://doi.org/10.1016/j.scitotenv.2018.10.374.

Russell, K.L., Vietz, G.J., Fletcher, T.D., 2020. How urban stormwater regimes drive geomorphic degradation of receiving streams. Prog. Phys. Geogr. Earth Environ. 44, 746–778. https://doi.org/10.1177/0309133319893927.

Schuler, M.S., Cañedo-Argüelles, M., Hintz, W.D., Dyack, B., Birk, S., Relyea, R.A., 2019. Regulations are needed to protect freshwater ecosystems from salinization. Philos. Trans. R. Soc. B Biol. Sci. 374. https://doi.org/10.1098/rstb.2018.0019.

Sherriff, S.C., Rowan, J.S., Fenton, O., Jordan, P., Melland, A.R., Mellander, P.E., Huallacháin, D., 2016. Storm event suspended sediment-discharge hysteresis and controls in agricultural watersheds: implications for watershed scale sediment management. Environ. Sci. Technol. 50, 1769–1778. https://doi.org/10.1021/acs.est.5b04573.

Sherriff SC, Rowan JS, Fenton O, Jordan P, Ó hUallacháin D (2019) Influence of land management on soil erosion, connectivity and sediment delivery in agricultural catchments: closing the sediment budget. L. Degrad. Dev. 44:. doi: https://doi.org/10.1002/ldr.3413.

StormWatch, 2020. StormWatch ALERT Flood Warning System. https://www.stormwatch.com/home.php (Accessed 1 Jan 2020).

Tang, Weigang, Carey, Sean K., 2017. HydRun: a MATLAB toolbox for rainfall–runoff analysis. Hydrol. Process. 31 (15), 2670–2682.

Tunqui Neira, J.M., Tallec, G., Andréassian, V., Mouchel, J.-M., 2020. A combined mixing model for high-frequency concentration–discharge relationships. J. Hydrol. 591, 125559. https://doi.org/10.1016/j.jhydrol.2020.125559.

United States Census Bureau (2007) TIGER/Line Shapefiles. https://www.census.gov/geographies/mapping-files/time-series/geo/tiger-line-file.html. Accessed 1 Jan 2021.

Vaughan, M.C.H., Bowden, W.B., Shanley, J.B., Vermilyea, A., Sleeper, R., Gold, A.J., Pradhanang, S.M., Inamdar, S.P., Levia, D.F., Andres, A.S., Birgand, F., Schroth, A.W., 2017. High-frequency dissolved organic carbon and nitrate measurements reveal differences in storm hysteresis and loading in relation to land cover and seasonality. Water Resour. Res. 53, 5345–5363. https://doi.org/10.1002/2017WR020491.

Vercruysse, K., Grabowski, R.C., Rickson, R.J., 2017. Suspended sediment transport dynamics in rivers: multi-scale drivers of temporal variation. Earth-Sci. Rev. 166, 38–52. https://doi.org/10.1016/j.earscirev.2016.12.016.

Waterman, B.R., Alcantar, G., Thomas, S.G., Kirk, M.F., 2022. Spatiotemporal variation in runoff and baseflow in watersheds located across a regional precipitation gradient. J. Hydrol. Reg. Stud. 41, 101071. https://doi.org/10.1016/j.ejrh.2022.101071.

Whitney, J.W., Glancy, P.A., Buckingham, S.E., Ehrenberg, A.C., 2015. Effects of rapid urbanization on streamflow, erosion, and sedimentation in a desert stream in the American Southwest. Anthropocene 10, 29–42. https://doi.org/10.1016/j.ancene.2015.09.002.

Wymore, A.S., Leon, M.C., Shanley, J.B., McDowell, W.H., 2019. Hysteretic response of solutes and turbidity at the event scale across forested tropical montane watersheds. Front. Earth Sci. 7, 1–13. https://doi.org/10.3389/feart.2019.00126.

Yang, W., Xiao, C., Zhang, Z., Liang, X., 2021. Can the two-parameter recursive digital filter baseflow separation method really be calibrated by the conductivity mass balance method? Hydrol. Earth Syst. Sci. 25 (4), 1747–1760.

Zaimes, G., Tamparopoulos, A.E., Tufekcioglu, M., Schultz, R.C., 2021. Understanding stream bank erosion and deposition in Iowa, USA: a seven year study along streams in different regions with different riparian land-uses. J. Environ. Manag. 287, 112352. https://doi.org/10.1016/j.jenvman.2021.112352.

Zarnaghsh, A., Husic, A., 2021. Degree of anthropogenic land disturbance controls fluvial sediment hysteresis. Environ. Sci. Technol. 55, 13737–13748. https://doi.org/10.1021/acs.est.1c00740.

Zimmer, M.A., Pellerin, B., Burns, D.A., Petrochenkov, G., 2019. Temporal variability in nitrate-discharge relationships in large rivers as revealed by high-frequency data. Water Resour. Res. 55. https://doi.org/10.1029/2018WR023478.

Zuecco, G., Penna, D., Borga, M., van Meerveld, H.J., 2016. A versatile index to characterize hysteresis between hydrological variables at the runoff event timescale. Hydrol. Process. 30, 1449–1466. https://doi.org/10.1002/hyp.10681.